The largest aftershock: How strong, how far away, how delayed?

M. Tahir,[1] J.-R. Grasso,[1] and D. Amorèse[2]

Received 15 December 2011; revised 18 January 2012; accepted 18 January 2012; published 17 February 2012.

[1] Proposed in the 1950's, Båth's law states that the largest aftershock has a magnitude that is typically 1.2 less than that of the mainshock. Thirty years of the global earthquake catalog allow us to extend Båth's law in time, space and focal mechanism. On average, reverse faults have a smaller magnitude and distance from the mainshock to largest aftershock than strike-slip faults. The distribution of the time intervals between mainshocks and their largest aftershocks obeys power law, but with a somewhat faster rate of decay than for aftershocks, in general. This implies that the largest aftershocks are more likely to occur earlier rather than later in a given sequence of aftershocks.
Citation: Tahir, M., J.-R. Grasso, and D. Amorèse (2012), The largest aftershock: How strong, how far away, how delayed?, *Geophys. Res. Lett.*, *39*, L04301, doi:10.1029/2011GL050604.

1. Introduction

[2] Earthquakes are the brittle response of the earth crust to stress–strain changes. These brittle seismic instabilities in the crust emerge as combined and complex effects of the response of heterogeneous media to small changes in loading rate which occur over a wide range of scales [e.g., *Bak and Tang*, 1989; *Sornette and Sornette*, 1989; *Main*, 1995; *Rundle et al.*, 2003]. These brittle deformations scale from dislocations and microcracks ($\sim$1 μm to 1 cm) to tectonic plate boundaries (10^3–10^4 km), whereas time scales range from a few seconds during dynamic rupture to 10^3–10^4 years (as the repeat times for the large $M > 7 - 8$ earthquakes) and to 10^7–10^8 years (evolution of the plate boundaries) [e.g., *Rundle et al.*, 2003]. For earthquakes, *Gutenberg and Richter* [1944] suggested the frequency magnitude distribution as;

$$log_{10}N = a - bM \tag{1}$$

where N is the total number of earthquakes with magnitude M or greater, a and b are constants. Regional analyses [e.g., *Utsu*, 2002] suggest b – *values* in the 0.8–1.2 range, including for aftershock sequences. Variation in b – *value* across different stress regimes are suggested by *Schorlemmer et al.* [2005]. Aftershocks also are observed to obey Omori's law [*Utsu*, 1961]

$$N(t) = \frac{K}{(t+c)^p}, \tag{2}$$

where $N(t)$ is the number of aftershocks per unit time, t is the elapsed time since the mainshock, K, c and p are constants. A median p – *value* of $\sim$1.1 is reported for the aftershock sequences in the various parts of the world, with a range of $\sim$0.6–2.5 [*Utsu et al.*, 1995]. *Narteau et al.* [2009] observed that c – *value* varied with mainshock faulting styles. As proposed by *Helmstetter and Sornette* [2003a]

$$K = 10^{\alpha(M-M_c)} \tag{3}$$

M_c is threshold magnitude for catalog completeness, α is a parameter that controls the relative number of aftershocks triggered as a function of mainshock magnitude($\alpha = 0.66 - 1.15$, suggested by *Hainzl and Marsan* [2008] for the global catalog). Thirdly Båth's law for earthquake aftershocks is observed in many empirical and statistical studies. Initially reported by *Richter* [1958] as Båth's observation, it states the average magnitude difference (ΔM) between the mainshock and its largest aftershock is 1.2, regardless of mainshock magnitude [*Båth*, 1965]. A number of studies have been conducted for the physical interpretation of Båth's law [e.g., *Vere-Jones*, 1969; *Console et al.*, 2003; *Helmstetter and Sornette*, 2003b; *Shcherbakov et al.*, 2006; *Vere-Jones*, 2008]. Among them *Helmstetter and Sornette* [2003b] using ETAS (epidemic type aftershock sequence for seismicity model) simulations provide a comprehensive analysis of the empirical Båth's law.

[3] They suggest that Båth's law occurrence depends on both α – *value* of the mainshock and the relative difference, ($M_m - M_c$), between mainshock magnitude (M_m) and catalog completeness (M_c) value. When $M_m - M_c \geq 2$ and $\alpha = 0.8 - 1.0$, then Båth's law applies. In other cases, i.e., $M_m - M_c < 2$, α-value < 0.8, $\langle \Delta M \rangle$ is smaller than 1.2 (i.e., ranging between 0 and 1.2) and it increases rapidly with M_m.

[4] In this latter case, the apparent increase in $\langle \Delta M \rangle$ is correlated with a low α – *value*. A lower aftershock rate implies a lower picking rate in the Gutenberg-Richter law distribution, and thus a lower probability of a large magnitude occurrence [see *Helmstetter and Sornette*, 2003b, equation 1]. More recently *Saichev and Sornette* [2005] showed the relationship of Båth's $\Delta M = 1.2$ value to the branching ratio (n) of the ETAS point process model of earthquake interactions. For high n ($n \geq 0.8$), α ($\alpha \geq 0.9$) values, the ETAS model yields a constant value of $\Delta M = 1.2$ (Båth's law) and for low n ($n \leq 0.6$) and α ($\alpha \leq 0.5$) Båth's law does not apply.

[5] In this paper we extend Båth's law, (i) to space and time patterns of the largest aftershocks, and (ii) we consider the earthquake faulting style as a possible control parameter on size and location of the largest aftershock. To do this, we explore $\Delta T = T_m - T_a$ (T_m = mainshock time, T_a = largest aftershock time) and $\Delta D^* = D_a^*$ is the normalized distance between the largest aftershock and the mainshock epicenter.

[6] Using the USGS global earthquake catalog, we verify that the ΔM, ΔT and ΔD^* values are independent of mainshock magnitude. Second, we investigate density distributions of size, time and space patterns of aftershocks.

[1]ISTerre, UJF-Grenoble, CNRS, Grenoble, France.
[2]M2C, UMR 6143, Université de Caen Basse-Normandie, CNRS, Caen, France.

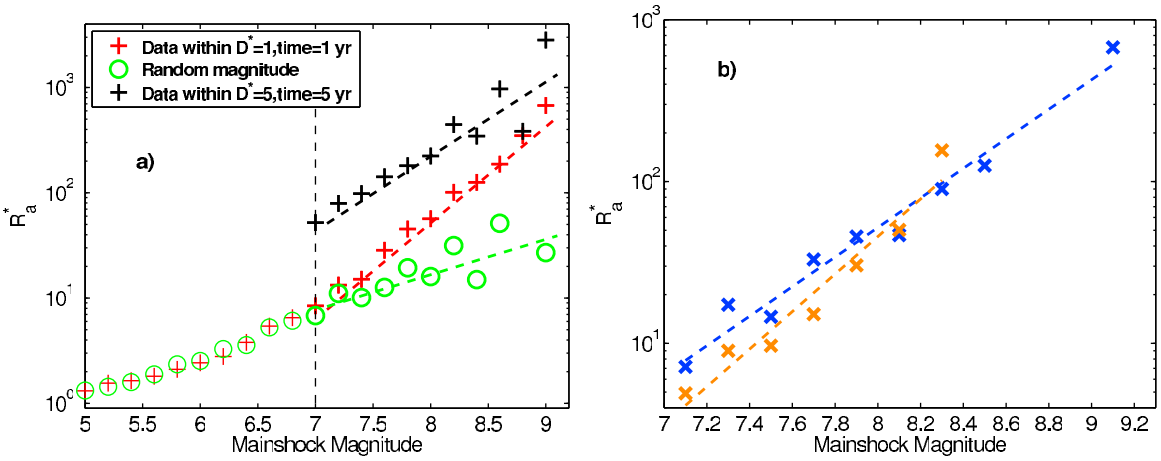

Figure 1. Aftershock normalised rate ($R^*_a = R_a/N_m$) as a function of mainshock size and faulting style: R_a is the number of aftershocks within mainshock magnitude class $\in [M_m, M_m + 0.2]$ for $M_m \geq 5$, N_m is the number of mainshocks. (a) Aftershock within 1 yr and $D^* = 1$ window (red cross), aftershock from randomly reshuffled magnitude catalog (green circle), aftershocks (black cross) within 5 yr, $D^* = 5$ window. The slope of the rate versus magnitude plot is defined as $\alpha - value$ [e.g., *Helmstetter*, 2003]. Note that the increase in $\alpha - value$ for $M_m > 7$ events, corresponds to $M_m - M_c \geq 2$. Below $M_m = 7$ $\alpha - value$ is close to 0.38 ± 0.03 for random and real data. Above $M_m = 7$, the slope value is 0.34 ± 0.08 and 0.91 ± 0.03 for random and real data respectively (see text for details). (b) Aftershock rate as a function of faulting style: reverse slip (blue cross, $\alpha = 0.91 \pm 0.06$); strike slip (orange cross, $\alpha = 1.16 \pm 0.12$). Note that the aftershock rates is always larger for reverse slip aftershocks than for strike slip aftershocks for $M_m < 8$.

Third, we analyse ΔM and ΔD^* values as functions of earthquake faulting styles, as defined according mainshock rake angle [e.g., *Aki and Richards*, 2002].

2. Data and Methods

[7] We selected shallow (depth < 70 km) earthquakes of the available global earthquake catalog, (1973–2010, http://earthquake.usgs.gov) with M_s (surface wave magnitude) $\geq M_c$ (threshold magnitude). For the selection of aftershocks and mainshocks, the completeness magnitude M_c is computed for the entire USGS catalog containing all earthquakes. Using median-based analysis of the segment slope (MBASS) method [*Amorese*, 2007], we derive $M_c = 5$, the same M_c value was previously reported by *Kagan and Jackson* [2010]. Focal mechanism solutions are taken from global Harvard CMT catalog (http://earthquake.usgs.gov/earthquakes/eqarchives/sopar/), 1977–2010.

[8] A number of declustering procedures are available to isolate aftershocks from background seismicity [e.g., *Gardner and Knopoff*, 1974; *Reasenberg*, 1985; *Kagan*, 1991; *Knopoff*, 2000; *Felzer et al.*, 2004; *Helmstetter et al.*, 2005; *Marsan and Lengline*, 2008]. None of them being 100% robust, we instead focus in the near field by selecting aftershocks as events which occur within one fault length (L) distance from the mainshock. By using normalized distance to mainshock as $D^* = |D/L|$, D is the aftershock distance to the mainshock, which is measured as the arc length on the earth's surface. L is the earthquake rupture length, derived from the earthquake magnitude, $L \sim 10^{0.59M_m}$ [*Wells and Coppersmith*, 1994, Table 2A]. We test how the patterns evolve when using $D^* = [1,2,\ldots5]$ and $[1,2,\ldots5]$ years for the space and time windows respectively (see auxiliary material).[1]

[9] For mainshock selection we follow *Helmstetter and Sornette* [2003b]; *Saichev and Sornette* [2005] who observed that Båth's law only exists for events whose $\alpha - value$ is larger than 0.5 (see equation (3)). This criterion corresponds to $M_m - M_c \geq 2$ [e.g., *Helmstetter and Sornette*, 2003b]. Because $M_c = 5$ for the global data, we expect a constant ΔM with respect to mainshock magnitude for $M_m \geq 7$ (Figures 1 and 2). To ensure the robustness of the $M_m - M_c \geq 2$ mainshock selection, we estimate $\alpha - value$ for the entire earthquake catalog and for the thrust, strike slip faulting styles (Figure 1a). We sum up the number of aftershocks within time = 1 year, $D^* = 1$ window with mainshock magnitude $\in [M_m, M_m + 0.1]$ bin and we further normalize by the number of mainshocks in each bin. The least square estimate of the slope value is defined as the α value. Accordingly, Figure 1 suggests $M_m \geq 7$ as the threshold value for events with $\alpha \geq 0.5$.

[10] First, we compute magnitude difference (ΔM), time (ΔT) and normalized distance (ΔD^*) between mainshock and largest aftershock as a function of mainshock magnitude classes $[M_m, M_m + 0.1]$ for $M_m = 7$–9.5. Then average, standard deviation and median with first and third quartiles (Q1,Q3) are being determined for each of the magnitude classes. Quartiles provide an interesting measure of the data dispersion since they are less susceptible than standard deviation when the data distribution is skewed or has many outliers. Because above $M = 8.3$ and for normal events, there is at most 1 single event per magnitude bin, we cannot compute error bars. Using $M_m \geq 7$, in the global catalog we only have 26 normal faulting events for 100 and 191 strike slip and thrust events, respectively. Accordingly, we restrict the following analysis to $M \leq 8.3$ of strike slip and reverse faulting earthquakes.

[11] Second, the density distribution of magnitude (ΔM), time (ΔT) and average linear density [e.g., *Felzer and Brodsky*, 2006] of normalized distance (ΔD^*) between

[1]Auxiliary materials are available in the HTML. doi:10.1029/2011GL050604.

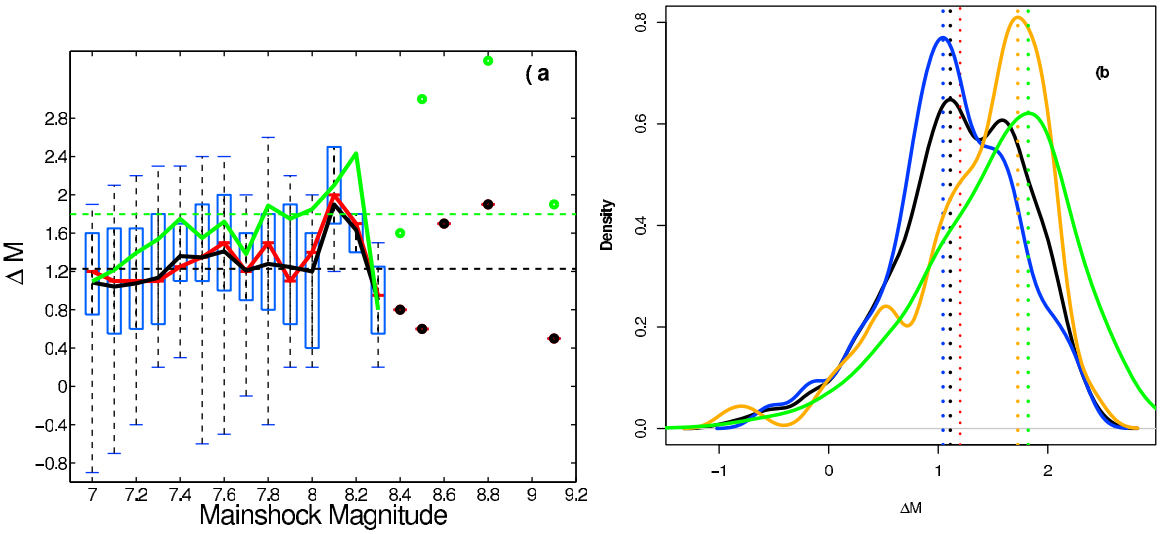

Figure 2. Magnitude difference (ΔM) between mainshock and its corresponding largest aftershock. (a) Average (black), median ΔM (red) and average ΔM for reshuffled magnitude (green). Vertical blue box plots lower quartile (Q1), and upper quartile (Q3). Horizontal dotted lines are global average for data and reshuffled magnitude (b) ΔM distribution for different faulting styles. All type of mainshock (black), reverse events (blue), strike slip (orange) and reshuffled magnitude (green). Dotted vertical lines are mode values, and red vertical line is Båth's law. Aftershocks are selected within time = 1 year and $D^* = 1$. Because above $M = 8.3$ there is at most 1 single event per magnitude bin, we cannot compute error bars.

mainshock and the largest aftershock are analyzed. In order to test the stability of the results, we compare each of ΔM, ΔT and ΔD^* outputs against the one derived from randomly reshuffled magnitude, time and location, respectively (i.e., either magnitude or time or location of events within the catalog are randomly interchanged with each other). Each reshuffled data are averaged results from 100 simulations.

3. Results and Discussion

[12] For the global earthquakes catalog using $M_m \geq M_c + 2$, time ≤ 1 yr and $D^* \leq 1$ for time and space window, we observe $\alpha = 0.91 \pm 0.03$ (Figure 1). This value falls in the suggested range for Båth's law [e.g., *Helmstetter and Sornette*, 2003b; *Saichev and Sornette*, 2005].

[13] We showed that the normalized aftershock rate of reverse events remains higher than for strike slip events for $M_m < 8.0$ (Figure 1b). This pattern indicate more aftershocks for reverse than strike slip events.

[14] By selecting mainshock magnitude $\geq M_c + 2$ [*Helmstetter and Sornette*, 2003b; *Saichev and Sornette*, 2005] we first validated Båth's law for world wide earthquake catalog, i.e., average $\Delta M \sim 1.2$, independent of the mainshock magnitude (Figure 2) and second, we extend this empirical law to distance (ΔD^*) and time (ΔT), (Figures 3 and 4). The average density distribution of ΔM is

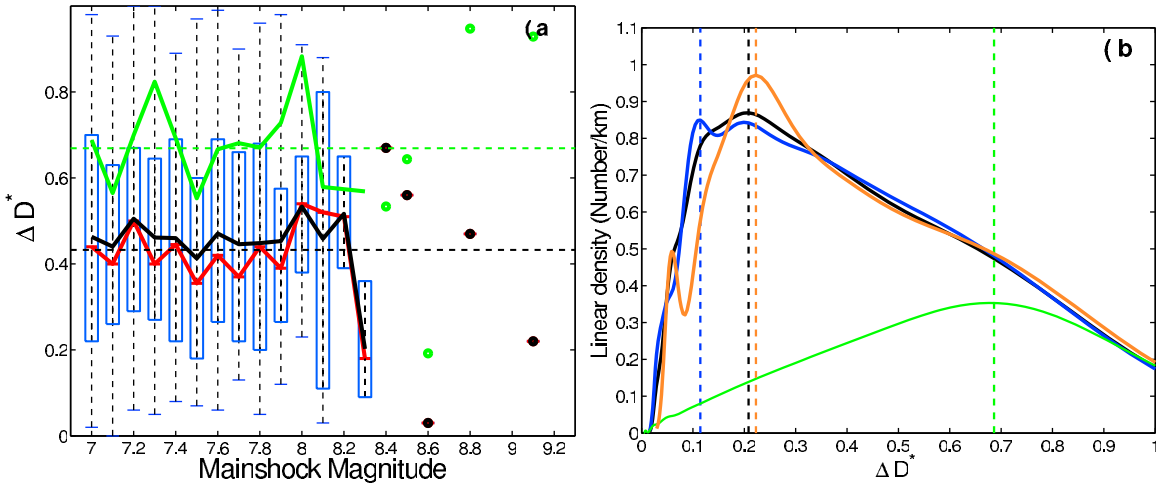

Figure 3. Normalized distance difference (ΔD^*) between mainshock and its corresponding largest aftershock. (a) Average ΔD^* (black), median ΔD^* (red) and average ΔD^* for reshuffled location (green). Vertical blue box plots lower quartile (Q1), and upper quartile (Q3). Horizontal dotted lines are global average for data and reshuffled location. (b) linear density distribution of ΔD^* for different faulting styles, with all type (black), reverse events (blue), strike slip (orange) and reshuffled location (green). Same as Figure 2 but for data selection.

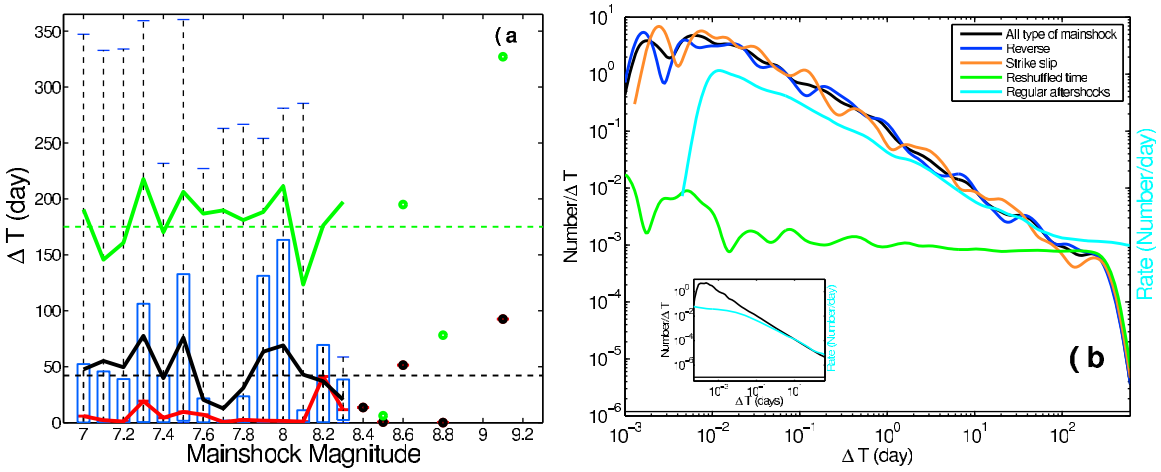

Figure 4. Time difference (ΔT) between mainshock and its corresponding largest aftershock. (a) Average (black), median (red) and average ΔT for reshuffled time (green). Horizontal dotted lines are global average. Vertical blue box plots lower quartile (Q1), and upper quartile (Q3). (b) ΔT distribution of largest aftershock for different faulting styles. Slope of the ΔT distribution for all type, reverse and strike slip events are respectively 0.96 ± 0.03, 0.96 ± 0.04 and 0.98 ± 0.05. Relaxation rate (sky blue) for regular aftershock (not restricted to the largest one) corresponds to $p - value$ = 0.82 ± 0.009. Insert in Figure 4b is the average of 1000 ETAS model simulations with input p = 1.2 and n = 0.99, (n is the branching ratio [e.g., *Helmstetter and Sornette*, 2003b]). Black line is the ΔT distribution for the largest aftershock from synthetic catalog, slope = 0.85 ± 0.027 and light blue is the Omori's law for all aftershocks, $p - value$ = 1.05 ± 0.0008.

not gaussian as it shows a fat tail, reminiscent of the Gutenberg Richter law (Figure 2b and S1e). Furthermore, the ΔM distribution is faulting style dependent i.e., mode of $\Delta M_{ss} > \Delta M_r$ (1.51, 0.95, ΔM_{ss}, ΔM_r being magnitude difference between mainshock and largest aftershock for strike slip and reverse events respectively). Accordingly, we expect on average $\Delta M_{ss} - \Delta M_r$ = 0.24, i.e., a 0.24 magnitude decrease for the largest aftershock of strike slip mainshocks relatively to reverse events. This 0.24 average magnitude decrease is within the $\langle \Delta M \rangle$ = 0.19–0.33 range of analytical ΔM estimates as a function of aftershock rate and $b - value$ [*Feller*, 1966; *Helmstetter and Sornette*, 2003b]. From equation (1) and (4) of *Helmstetter and Sornette* [2003b] we derived $\langle \Delta M \rangle_r - \langle \Delta M \rangle_{ss} \sim \frac{1}{b_r} \log_{10} \frac{N_r}{N_m} - \frac{1}{b_{ss}} \log_{10} \frac{N_{ss}}{N_m}$. For these $\langle \Delta M \rangle$ estimates we use $b - value$ b_r = 0.99 ± 0.06, b_{ss} = 1.12 ± 0.09 as estimated for global CMT catalog by M. Tahir and J. Grasso (Faulting style controls on the Omori law parameters from global earthquake catalogs, submitted to *Journal of Geophysical Research*, 2012).

[15] The average linear density distribution of ΔD^* is strongly peaked at ΔD^* = 0.2, with mode values for $\Delta D^*_{ss} > \Delta D^*_r$ (Figure 3). Accordingly, the largest aftershocks of strike slip mainshocks are on average, smaller than and occur at a larger distance from the mainshock than those triggered by reverse shocks (Figures 2 and 3).

[16] For any magnitude bin, the rate of aftershocks is always larger for reverse triggers than for strike slip triggers (Figure 1b). *Tahir and Grasso* [2009, submitted manuscript, 2012] suggested this global production of aftershock is driven by a lower $p - value$, larger $K - value$, for reverse events than that for strike slip events, respectively. For fixed $b - value$, a larger aftershock rate imply a greater probability to randomly pick a large earthquake from Gutenberg-Richter law [see][as predicted by ETAS model *Helmstetter et al.*, 2003]. Accordingly, the larger aftershock rate we resolve for $M_m \geq 7.0$ on Figure 1b drives the larger magnitude which emerges for the largest aftershocks of reverse events than for strike slip events, respectively. Also, one must note the lower α value we resolve for reverse earthquakes than for strike slip ones further re-enforces this pattern, with $\langle \Delta M \rangle$ = f($b - \alpha/b$, M_m, K/1-n) as derived from analytical solution of ETAS model [e.g., *Helmstetter and Sornette*, 2003b, equation (5)]. For the distance patterns, it appears that in the near field, within 1–3 fault length of the mainshock, the aftershocks are driven by the co-seismic static stress changes [*Kanamori and Brodsky*, 2004; *Parsons and Velasco*, 2009; *Hainzl et al.*, 2010; *Marsan and Lengliné*, 2010]. Accordingly, most of strike-slip aftershock epicenters are observed to be clustered at the fault edges, i.e., at larger distance and more clustered than the rough plateau density of reverse aftershock epicenters which are located within the hanging wall [*King et al.*, 1994; *Stein*, 1999; *Freed*, 2005]. We find that the ΔT distribution is independent of faulting style and obeys power law. The observed 0.2 slope difference between inter-event time of the largest aftershock and regular aftershock relaxation is found to emerge from synthetic catalogs (Figure 4b, inset) using epidemic cascading point process (ETAS) for earthquake interactions [e.g., *Helmstetter et al.*, 2003].

4. Conclusions

[17] Thirty years of the global earthquake catalog allow us to extend Båth's law in time, space and focal mechanism. First, more aftershocks are observed for reverse than for strike slip events. Second, for reverse faults the ΔM of largest aftershock is in average smaller than the one of strike slip events, all being independent of magnitude. Third the distance from the mainshock to the largest aftershock is somewhat less for reverse faults than for strike slip faults. Fourth, the distribution of time intervals between mainshocks and their largest aftershocks is consistent with power

law but with a somewhat faster rate of decay than for aftershocks in general. This implies that the largest aftershock is more likely to occur earlier than later in a given sequence of aftershocks (i.e., median $\Delta T \sim 3$ days).

[18] These empirical results for, ΔM, ΔD^*, ΔT are robust patterns that are direct inputs to refine the current practice of early forecasts of earthquakes activity (http://www.cseptesting.org/).

[19] On the one hand, these results provides quantitative probabilistic prediction tools for time space and size estimates of the largest aftershock. On the other hand these predictions, size and distance dependent on the faulting style, argue for going beyond the point process for the cascading model of earthquake interactions. Our analysis of the largest aftershock patterns confirms the role of static triggering as the main process to trigger earthquake in the near field, i.e., within 1 year and 1 fault length of mainshock.

[20] **Acknowledgments.** This work is partially supported by the French ANR Pakistan program and the European Program TRIGS. M.T. is supported by the HEC – French Pakistan program. We acknowledge useful comments and discussion with A. Helmstetter, M. Bouchon. We greatly appreciate review of previous versions of the manuscript by A. McGarr, F. Grasso, M. Werner, A.P. Rathbun and two anonymous reviewers.

[21] The Editor thanks two anonymous reviewers for their assistance in evaluating this paper.

References

Aki, K., and P. Richards (2002), *Quantitative Seismology*, 2nd ed., Univ. Sci., Sausalito, Calif.

Amorese, D. (2007), Applying a change-point detection method on frequency-magnitude distributions, *Bull. Seismol. Soc. Am.*, *97*(5), 1742–1749.

Bak, P., and C. Tang (1989), Earthquakes as a self-organized critical phenomenon, *J. Geophys. Res.*, *94*(B11), 15,635–15,637.

Båth, M. (1965), Lateral inhomogeneities of the upper mantle, *Tectonophysics*, *2*(6), 483–514.

Console, R., A. M. Lombardi, M. Murru, and D. Rhoades (2003), Båth's law and the self-similarity of earthquakes, *J. Geophys. Res.*, *108*(B2), 2128, doi:10.1029/2001JB001651.

Feller, W. (1966), *An Introduction to Probability Theory and Applications.*, vol. 2, Wiley, New York.

Felzer, K., R. Abercrombie, and G. Ekström (2004), A common origin for aftershocks, foreshocks, and multiplets, *Bull. Seismol. Soc. Am.*, *94*(1), 88–99.

Felzer, R., and E. Brodsky (2006), Decay of aftershock density with distance indicates triggering by dynamic stress, *Nature*, *441*, 735–738.

Freed, A. (2005), Earthquake triggering by static, dynamic, and postseismic stress transfer, *Annu. Rev. Earth Planet. Sci.*, *33*, 335–367.

Gardner, J., and L. Knopoff (1974), Is the sequence of earthquakes in southern california, with aftershocks removed, poissonian, *Bull. Seismol. Soc. Am.*, *64*(5), 1363–1367.

Gutenberg, B., and C. Richter (1944), Frequency of earthquakes in California, *Bull. Seismol. Soc. Am.*, *34*(4), 185–188.

Hainzl, S., and D. Marsan (2008), Dependence of the Omori-Utsu law parameters on main shock magnitude: Observations and modeling, *J. Geophys. Res.*, *113*, B10309, doi:10.1029/2007JB005492.

Hainzl, S., G. B. Brietzke, and G. Zöller (2010), Quantitative earthquake forecasts resulting from static stress triggering, *J. Geophys. Res.*, *115*, B11311, doi:10.1029/2010JB007473.

Helmstetter, A. (2003), Is earthquake triggering driven by small earthquakes?, *Phys. Rev. Lett.*, *91*(5), 058501, doi:10.1103/PhysRevLett.91.058501.

Helmstetter, A., and D. Sornette (2003a), Importance of direct and indirect triggered seismicity in the ETAS model of seismicity, *Geophys. Res. Lett.*, *30*(11), 1576, doi:10.1029/2003GL017670.

Helmstetter, A., and D. Sornette (2003b), Båth's law derived from the Gutenberg-Richter law and from aftershock properties, *Geophys. Res. Lett.*, *30*(20), 2069, doi:10.1029/2003GL018186.

Helmstetter, A., D. Sornette, and J.-R. Grasso (2003), Mainshocks are aftershocks of conditional foreshocks: How do foreshock statistical properties emerge from aftershock laws, *J. Geophys. Res.*, *108*(B1), 2046, doi:10.1029/2002JB001991.

Helmstetter, A., Y. Y. Kagan, and D. D. Jackson (2005), Importance of small earthquakes for stress transfers and earthquake triggering, *J. Geophys. Res.*, *110*, B05S08, doi:10.1029/2004JB003286.

Kagan, Y. (1991), Likelihood analysis of earthquake catalogues, *Geophys. J. Int.*, *106*(1), 135–148.

Kagan, Y., and D. Jackson (2010), Earthquake forecasting in diverse tectonic zones of the globe, *Pure Appl. Geophys.*, *167*(6), 709–719.

Kanamori, H., and E. Brodsky (2004), The physics of earthquakes, *Rep. Prog. Phys.*, *67*, 1429–1496.

King, G., R. Stein, and J. Lin (1994), Static stress changes and the triggering of earthquakes, *Bull. Seismol. Soc. Am.*, *84*(3), 935–953.

Knopoff, L. (2000), The magnitude distribution of declustered earthquakes in Southern california, *Proc. Natl. Acad. Sci. U. S. A.*, *97*(22), 11,880–11,884.

Main, I. (1995), Earthquakes as critical phenomena: implications for probabilistic seismic hazard analysis, *Bull. Seismol. Soc. Am.*, *85*(5), 1299–1308.

Marsan, D., and O. Lengline (2008), Extending earthquakes' reach through cascading, *Science*, *319*(5866), 1076–1079.

Marsan, D., and O. Lengliné (2010), A new estimation of the decay of aftershock density with distance to the mainshock, *J. Geophys. Res.*, *115*, B09302, doi:10.1029/2009JB007119.

Narteau, C., S. Byrdina, P. Shebalin, and D. Schorlemmer (2009), Common dependence on stress for the two fundamental laws of statistical seismology, *Nature*, *462*(7273), 642–645.

Parsons, T., and A. A. Velasco (2009), On near-source earthquake triggering, *J. Geophys. Res.*, *114*, B10307, doi:10.1029/2008JB006277.

Reasenberg, P. (1985), Second-order moment of central california seismicity, 1969–1982, *J. Geophys. Res.*, *90*(B7), 5479–5495.

Richter, C. (1958), *Elementary Seismology*, pp. 611–618, W. H. Freeman, San Francisco, Calif.

Rundle, J. B., D. L. Turcotte, R. Shcherbakov, W. Klein, and C. Sammis (2003), Statistical physics approach to understanding the multiscale dynamics of earthquake fault systems, *Rev. Geophys.*, *41*(4), 1019, doi:10.1029/2003RG000135.

Saichev, A., and D. Sornette (2005), Distribution of the largest aftershocks in branching models of triggered seismicity: Theory of the universal Båth law, *Phys. Rev. E.*, *71*(5), 056127, doi:10.1103/PhysRevE.71.056127.

Schorlemmer, D., S. Wiemer, and M. Wyss (2005), Variations in earthquake-size distribution across different stress regimes, *Nature*, *437*(7058), 539–542.

Shcherbakov, R., D. Turcotte, and J. Rundle (2006), Scaling properties of the parkfield aftershock sequence, *Bull. Seismol. Soc. Am.*, *96*(4B), S376–S384.

Sornette, D., and A. Sornette (1989), Self-organised criticality and earthquakes, *Europhys. Lett.*, *9*, 197–202.

Stein, R. (1999), The role of stress transfer in earthquake occurrence, *Nature*, *402*(6762), 605–609.

Tahir, M., and J. Grasso (2009), Triggered earthquakes and earthquake interactions: The role of the focal mechanisms, *Eos Trans. AGU*, *90*(52), Fall Meet. Suppl., Abstract S51C-1438.

Utsu, T. (1961), A statistical study on the occurrence of aftershocks, *Geophys. Mag.*, *30*(4), 521–605.

Utsu, T. (2002), Statistical features of seismicity, in *International Handbook of Earthquake and Engineering Seismology*, *Int. Geophys. Ser.*, vol 81A, pp. 719–732, Academic, Amsterdam.

Utsu, T., Y. Ogata, and R. Matsu'ura (1995), The centenary of the Omori formula for a decay law of aftershock activity, *J. Phys. Earth*, *43*(1), 1–33.

Vere-Jones, D. (1969), A note on the statistical interpretation of Bath's law, *Bull. Seismol. Soc. Am.*, *59*(4), 1535–1541.

Vere-Jones, D. (2008), A limit theorem with application to Båth's law in seismology, *Adv. Appl. Probab.*, *40*(3), 882–896.

Wells, D. L., and K. J. Coppersmith (1994), New empirical relationships among magnitude, rupture length, rupture width, rupture area, and surface displacement, *Bull. Seismol. Soc. Am.*, *84*(4), 974–1002.

D. Amorèse, M2C, UMR 6143, Université de Caen Basse-Normandie, CNRS, 24 rue des Tilleuls, F-14000 Caen CEDEX, France.

J.-R. Grasso and M. Tahir, ISTerre, UJF-Grenoble, BP 53, F-38401 Grenoble CEDEX 9, France. (tahirm@obs.ujf-grenoble.fr)